

## **The Influence of annealing temperature on Structural and Optical Properties for thin ZnO Films Prepared by pulse laser deposition**

**تأثير درجة حرارة التلدين على الخصائص التركيبية والبصرية لغشاء أوكسيد  
الزركون المحضر بطريقة الترسيب بالليزر النبضي**

Mohammed A. Kadhim<sup>(a)</sup>      Mohammed O. Salman<sup>(b)</sup>

[a] College of Science, University of Karbala

[b] Ministry of Science and technology-mohammedoudah@yahoo.com

### **Abstract:**

In this work, structural and optical properties for thin ZnO films prepared by pulse laser deposition technique, on glass substrates, have been studied as a function of annealing temperature. This study shows that the films have energy gap decreases from 3.26 eV to 3.14 with increasing  $T_a$  from RT to 673 K.

Keywords: ZnO, pulse laser deposition, optical properties, Structural properties.

### **الخلاصة :**

تم في هذا البحث دراسة الخصائص التركيبية والبصرية لأغشية أوكسيد الزركون و المحضرة بطريق الترسيب بالليزر النبضي على أرضيات زجاجية كدالة لدرجة حرارة التلدين . بينت هذه الدراسة أن الاغشية تمتلك فجوة طاقة تتغير من 3.26 الى 3.14 الكترون فولت عند زيادة درجة حرارة التلدين من درجة حرارة الغرفة الى 673 كلفن

### **Introduction**

Zinc oxide (ZnO) is an important electronic and photonic material because of its wide-band semiconductor with a band gap of about to 3.37eV and large exciton binding energy of 60meV of excitons at room temperature [1-3].

ZnO can exist in three phases (a) hexagonal (wurtzite) [4] (b) zinc-blend [5] (c) rock salt [5]. The most stability ZnO structure is hexagonal (wurtzite) as shown in figure (1-2) with lattice parameters  $a=0.325\text{nm}$  and  $c=0.521\text{nm}$ .

Many different techniques such as chemical vapor deposition, organic chemical vapor deposition (MOCVD), plasma-assisted molecular beam epitaxy (PA-MBE), pulsed laser deposition (PLD), and spray pyrolysis technique have been used to growth the ZnO [6-8].

Among the various thin film deposition techniques, pulse laser deposition is one of the simplest growth techniques to deposit high quality films and nanostructures under optimized conditions of variety of materials ranging from superconductors to semiconductors to dielectrics to metals and many more [9].

The average crystalline size (D) was calculated using Debye-Scherrer's formula:[10]

$$D = \frac{K\lambda}{\beta_{hkl}\cos\theta} \dots\dots\dots 1$$

where K is shape factor =0.9,  $\lambda$  is the X- ray wavelength= 1.5406Å,  $\beta_{hkl}$  is the full width at half maximum in( rad) and  $\theta$  is bragg angle .

The strain induced in powders due to crystal imperfection and distortion ( $\varepsilon$ ) was calculated using the formula:

$$\varepsilon = \frac{\beta_{hkl}}{4 \tan\theta} \dots\dots\dots 2$$

From Equations 1 and 2, it was confirmed that the peak width from crystallite size varies as  $1/\cos\theta$  strain varies as  $\tan\theta$ . Assuming that the particle size and strain contributions to line

broadening are independent to each other and both have a Cauchy-like profile, the observed line breadth is simply the sum of Equations 1 and 2.

$$\beta_{hkl} = \frac{K\lambda}{D \cos\theta} + 4\epsilon \tan\theta \quad \dots\dots\dots 3$$

By rearranging the above equation, we get

$$\beta_{hkl} \cos\theta = \frac{K\lambda}{D} + 4\epsilon \sin\theta \quad \dots\dots\dots 4$$

The above equations are Williamson and Hall equations. A plot is drawn with  $4\epsilon \sin\theta$  along the x-axis and  $\beta_{hkl} \cos\theta$  along the y-axis, the crystalline size was estimated from the y-intercept, and the strain  $\epsilon$ , from the slope of the fit. In equation 4 the strain was assumed to be uniform in all crystallographic directions, thus considering the isotropic nature of the crystal, where the material properties are independent of the direction along which they are measured<sup>[11]</sup>

### **Experimental Procedure**

Pure zinc oxide powder with high purity (99.99%) were prepared by pressing under 5 Ton to formed a target with 2.5 cm diameter and 0.4 cm thickness. It should be as dense and homogenous as possible to ensure a good quality of the deposit.

Prior to deposit films, the glass substrates were cleaned in with commercial cleaner solution, distilled water and followed by alcohol using ultrasonic bath.

ZnO thin films were prepared using pulse laser deposition (PLD) technique which carried out inside a vacuum chamber generally at ( $10^{-3}$  Torr). The focused Nd:YAG (Huafei Tongda Technology—DIAMOND-288 pattern EPLS) SHG Q-switching beam (laser Power= 700 MJ,  $\lambda = 1064$  nm and  $f=6$ Hz) coming through a window is incident on the target surface making an angle of  $45^\circ$  with it. The substrate is placed in front of the target with its surface parallel to that of the target. Sufficient gap is kept between the target and the substrate so that the substrate holder does not obstruct the incident laser beam.

The thickness of prepared films was about 150 nm which measured by Michelson interferometer. An optical transmittance and absorbance spectra were recorded, at room temperature, in the wavelength range 300-1100 nm using OPTIMA SP-3000 UV-VIS spectrophotometer.

### **Results and Discussion**

Fig. (1) shows the X-ray diffraction for as deposited ZnO films and annealed 473 and 673 K, this figure shows that when the films annealed they were convert from amorphous to polycrystalline structure. Table (1) shows the experiment and the standard peaks from International Centre for Diffraction Data (JCPDS) for Wurtzite (Hex.) ZnO crystal <sup>[12]</sup>, this table shows a good identical between them. The preferred peak for ZnO film located at  $2\theta$  about  $34.4^\circ$  for (002) plane. The peaks intensities increase with increase  $T_a$ . The grain size increased with increasing  $T_a$ .

In addition we can also see from table (1) an increasing in  $d_{hkl}$  with increasing  $T_a$  i.e., slightly shift in  $2\theta$  to lower values because increasing the grain size, i.e increase in lattice constant as shown in table (2).

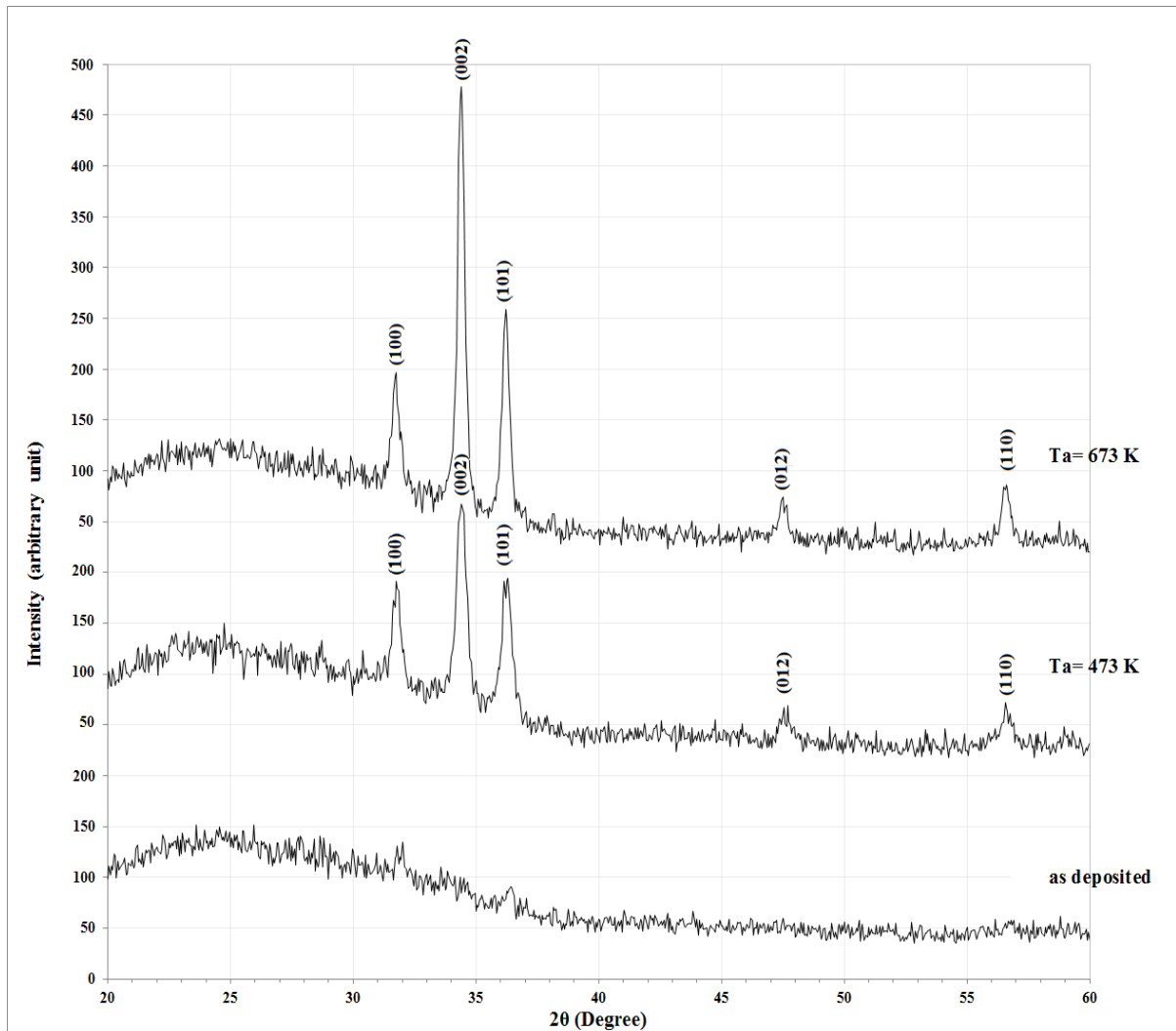


Fig. (1) X-ray diffraction patterns for as deposited and annealed ZnO films.

Table (1) Structural parameters :inter-planar spacing, crystalline size (by Sherrer's formula) for ZnO films.

| Ta (K)       | 2θ (Deg.) | FWHM (Deg.) | $d_{hkl}$ Exp.(Å) | G.S (nm) | $d_{hkl}$ Std.(Å) | hkl   |
|--------------|-----------|-------------|-------------------|----------|-------------------|-------|
| as deposited | -         | -           | -                 | -        | -                 | -     |
| 473          | 31.7612   | 0.4800      | 2.8151            | 17.2     | 2.8137            | (100) |
|              | 34.4154   | 0.4900      | 2.6038            | 17.0     | 2.6035            | (002) |
|              | 36.2492   | 0.5000      | 2.4762            | 16.7     | 2.4754            | (101) |
|              | 47.5327   | 0.5428      | 1.9114            | 16.0     | 1.9110            | (112) |
|              | 56.6026   | 0.5850      | 1.6247            | 15.4     | 1.6245            | (110) |
| 673          | 31.7542   | 0.3400      | 2.8157            | 24.3     | 2.8137            | (100) |
|              | 34.4011   | 0.3450      | 2.6049            | 24.1     | 2.6035            | (002) |
|              | 36.2477   | 0.3483      | 2.4763            | 24.0     | 2.4754            | (101) |
|              | 47.5298   | 0.3686      | 1.9115            | 23.6     | 1.9110            | (112) |
|              | 56.6011   | 0.3900      | 1.6248            | 23.1     | 1.6245            | (110) |

The lattice constants 'a' calculated from (100) peaks while 'c' from (002) peaks for Hex. ZnO films with different Ta using the following equation <sup>[13]</sup>

$$\frac{1}{d^2} = \frac{4}{3} \frac{h^2+hk+k^2}{a^2} + \frac{l^2}{c^2} \dots\dots\dots 5$$

Table (2) Comparison between standard and experimental lattice constants for hexagonal ZnO films.

| T <sub>a</sub> (K) | a (Å) Exp. | a (Å) Std. | c (Å) Exp. | c (Å) Std. |
|--------------------|------------|------------|------------|------------|
| 473                | 3.2506     | 3.2490     | 5.2076     | 5.2070     |
| 673                | 3.2513     | 3.2490     | 5.2097     | 5.2070     |

The calculated lattice constants decrease with annealing temperature and have a good agreement with standard card.<sup>[12]</sup>

The relation between  $\beta \cos(\theta)$  versus  $4\sin(\theta)$  was shown in fig (2). The slope for these lines represent the non-uniform strain and the y intersections represent  $(0.9\lambda/\text{Domain size})$  . The calculated values indicate that Domain size increase with increase T<sub>a</sub> from 473 to 673K, while the non-uniform strain decrease due to increasing the grain size.

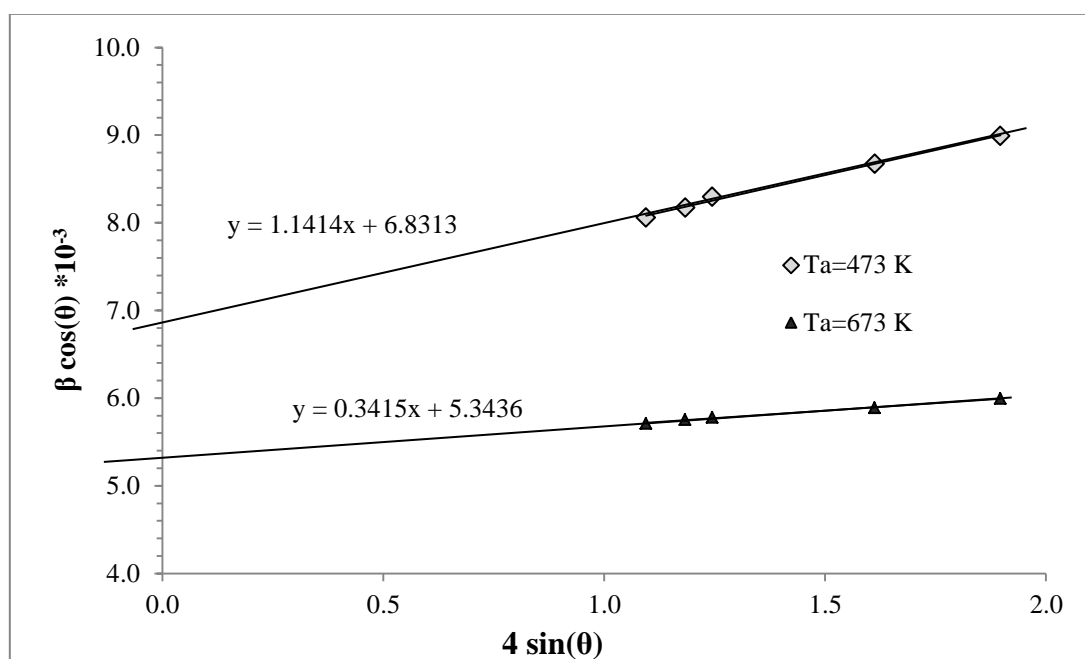


Fig. (2) Williamson and Hall relation for annealed ZnO films (T<sub>a</sub>=473 and 673)K.

Table (3) non-uniform strain and domain size for annealed ZnO films (T<sub>a</sub>=473 and 673)K.

| T <sub>a</sub> (K) | non-uniform strain*10 <sup>-3</sup> | Domain size (nm) |
|--------------------|-------------------------------------|------------------|
| 473                | 1.14                                | 20.3             |
| 673                | 0.34                                | 26.0             |

Optical measurements for ZnO films on glass substrate by pulse laser deposition with different annealing temperature (T<sub>a</sub>) was carried out in the wavelength range 300–1100 nm at room temperature (RT). Figure (3) shows the room temperature transmittance spectra for samples with different T<sub>a</sub>.

All spectra show good transparency, the transmittance pattern of all deposited thin films increases with increasing of wavelength ( $\lambda$ ). On the other hand the transmittance increases with the increase of T<sub>a</sub>. It is obvious from the figure that the transmittance for as deposited ZnO film at wavelength equal to 500nm was found to be 80.63%, and decrease to 72.07% when T<sub>a</sub> increase to 673 K.

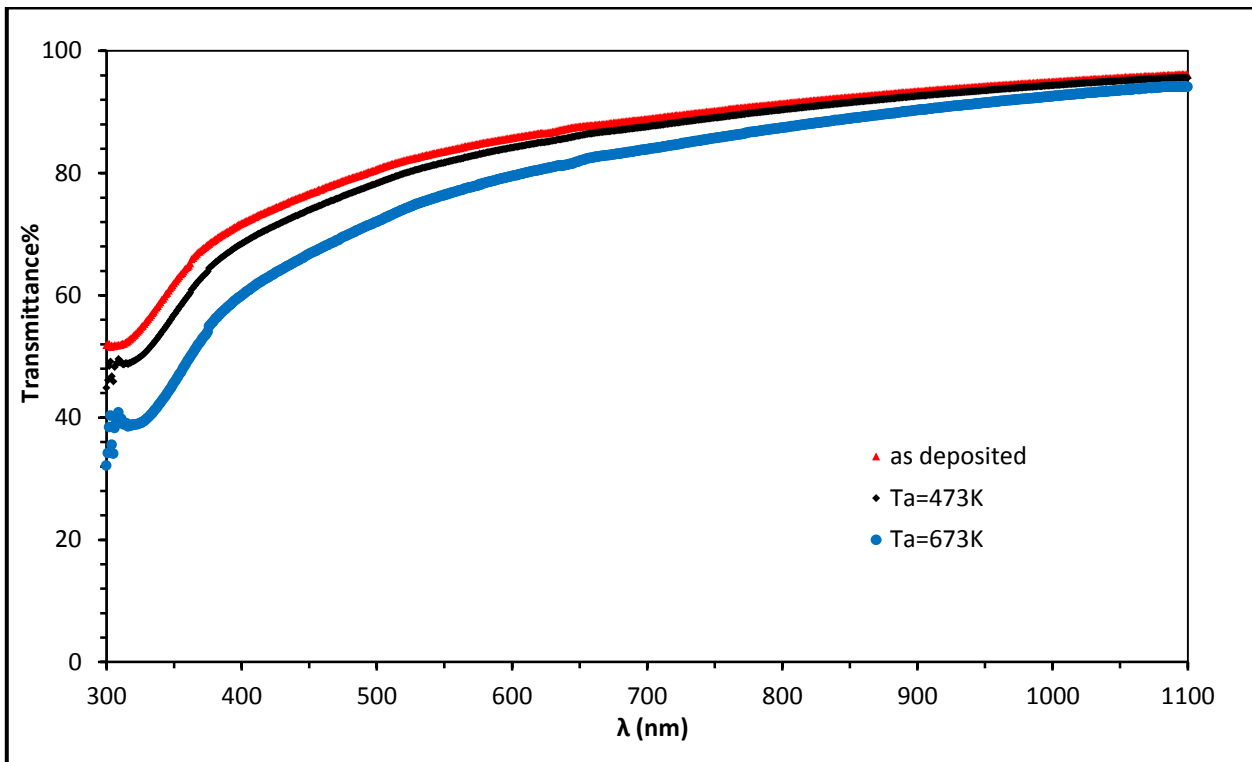


Fig.(3) Transmittance variation with the wavelength for as deposited and annealed ZnO films.

The absorption coefficient ( $\alpha$ ) of ZnO thin films was calculated from the optical transmittance spectrum measurements using the formula<sup>[14]</sup>:

$$\alpha = \frac{1}{t} \ln \left( \frac{1}{T} \right) \dots\dots\dots 5$$

where  $t$  is the thickness of thin films, and  $T$  is the transmittance intensity. The energy gap and optical constants were calculated for two samples.

The optical energy gap values ( $E_g^{opt}$ ) for thin ZnO films on glass have been determined by using Tauc equation<sup>[15]</sup>.

$$\alpha h\nu = A \left( h\nu - E_g \right)^r \dots\dots\dots 6$$

where  $h\nu$  is the photon energy,  $E_g$  is the optical band gap energy,  $A$  is inversely proportional to amorphousity and  $r$  is used to find the type of the optical transition by plotting the relations  $(\alpha h\nu)^{1/2}$ ,  $(\alpha h\nu)^{1/3}$ ,  $(\alpha h\nu)^{2/3}$ , and  $(\alpha h\nu)^2$  versus photon energy ( $h\nu$ ). The energy gap ( $E_g$ ) is then determined by the extrapolation of the linear portion at  $(\alpha h\nu)^2 = 0$ . It is found that the relation for  $r=1/2$  yields linear dependence part at which the absorption coefficient  $\alpha \geq 10^4 \text{ cm}^{-1}$ , which describes that ZnO film has the allowed direct transition.

The variation of  $(\alpha h\nu)^2$  as a function of photon energy for as deposited and annealed ZnO films. has been plotted in Fig. (4). This figure reveals that the annealing leads to decrease the energy gap from approximately 3.26 eV to 3.14 eV. This can be attributed to increase the grain size and which leads to decrease the strain causing increase in lattice constants.

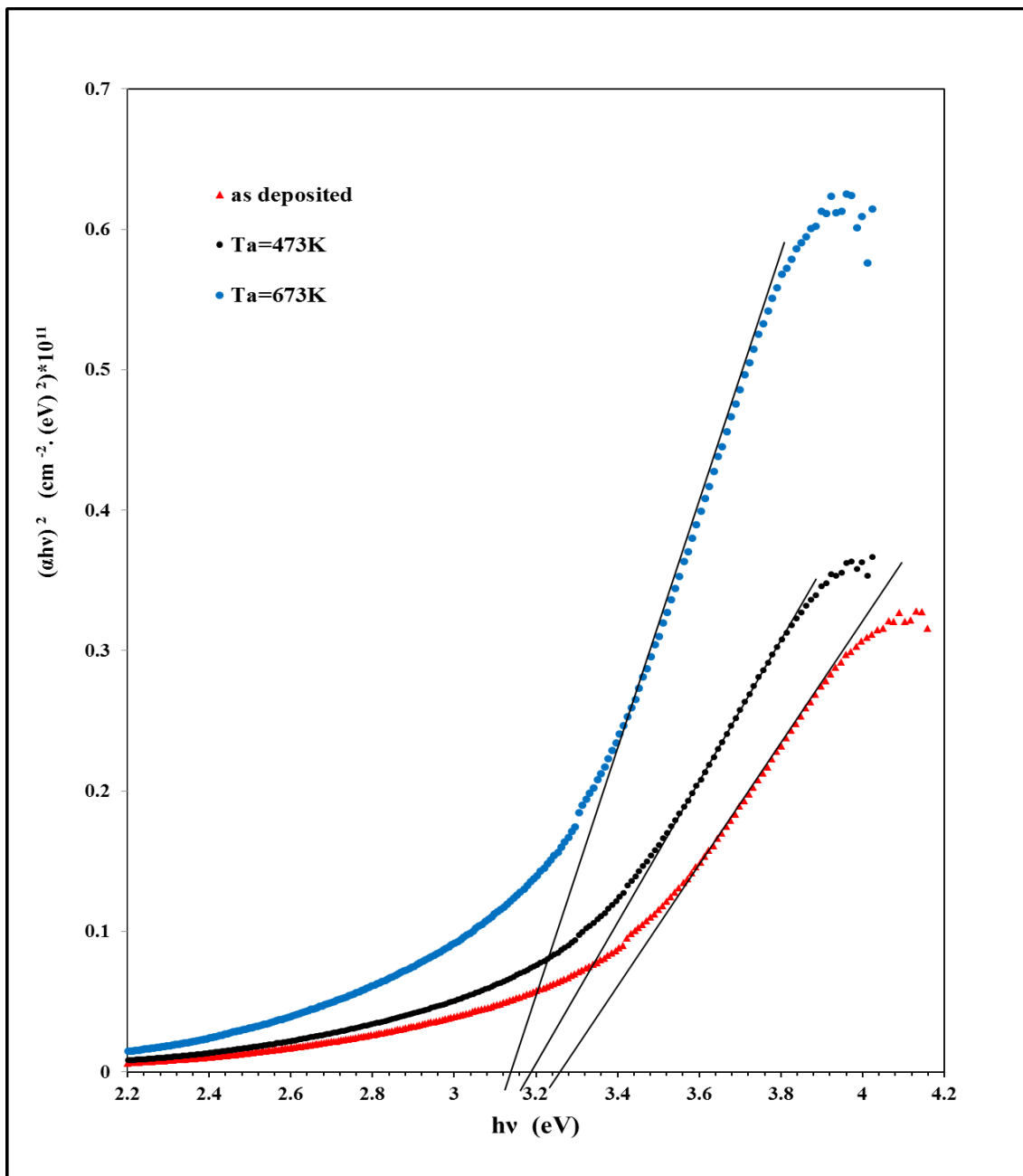


Fig.(4) The variation of  $(\alpha h\nu)^2$  versus photon energy ( $h\nu$ ) for as deposited and annealed ZnO films.

It is important to determine the optical constants of thin films such as refractive index ( $n$ ), extinction coefficient ( $k$ ), and the real ( $\epsilon_r$ ) and imaginary ( $\epsilon_i$ ) parts of dielectric constant.

Fig.(5) shows the variation of extinction coefficient ( $k = \alpha \lambda / 4\pi$ ) with wavelength) for as deposited and annealed ZnO films. The extinction coefficient depends mainly on absorption coefficient; for this reason, the behavior of it is similar for absorption coefficient i.e., the increasing of extinction coefficient with increasing photon energy because the absorption is increased and the peak shift to higher wavelength (red shift) with annealing.

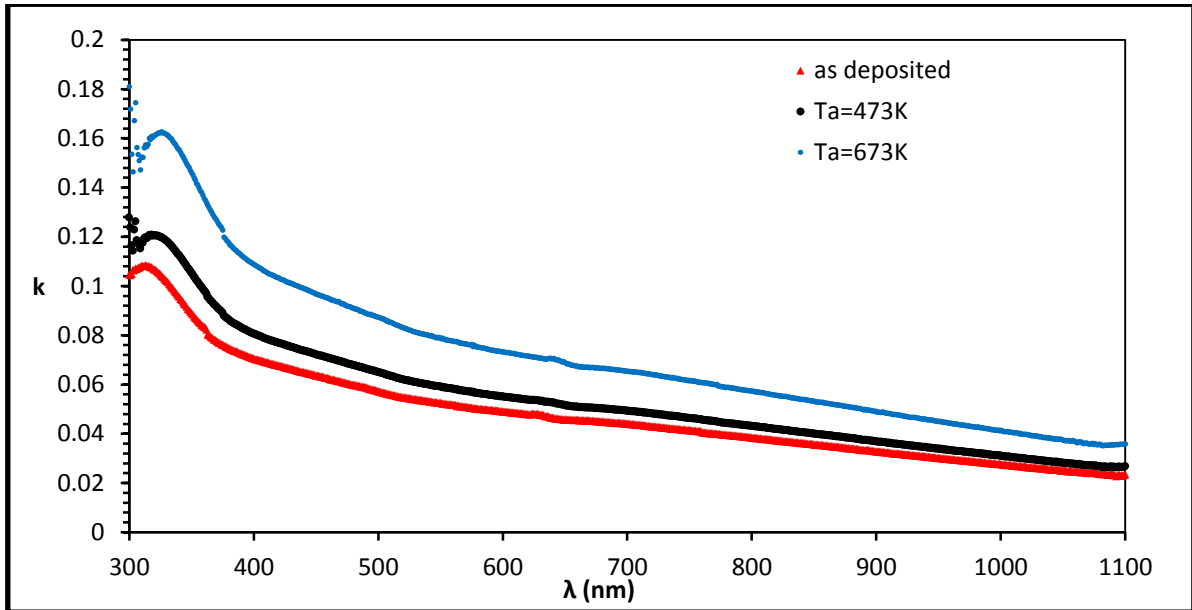


Fig. (5) Extinction coefficient versus wavelength for as deposited and annealed ZnO films.

The index of refraction for as deposited and annealed ZnO films was estimated from the reflectance (R) data using the relation <sup>[16]</sup>.

$$n = \sqrt{\frac{4R}{(1-R)^2} - k^2} - \frac{R+1}{R-1} \dots\dots\dots 7$$

The variation of the refractive index versus wavelength in the range 300–1100 nm, for as deposited and annealed ZnO films on glass. has been shown in Fig. (5). It is clear from this figure that the refractive index in general increases with increasing of annealing temperature. This behavior is due to the decrement in energy gap.

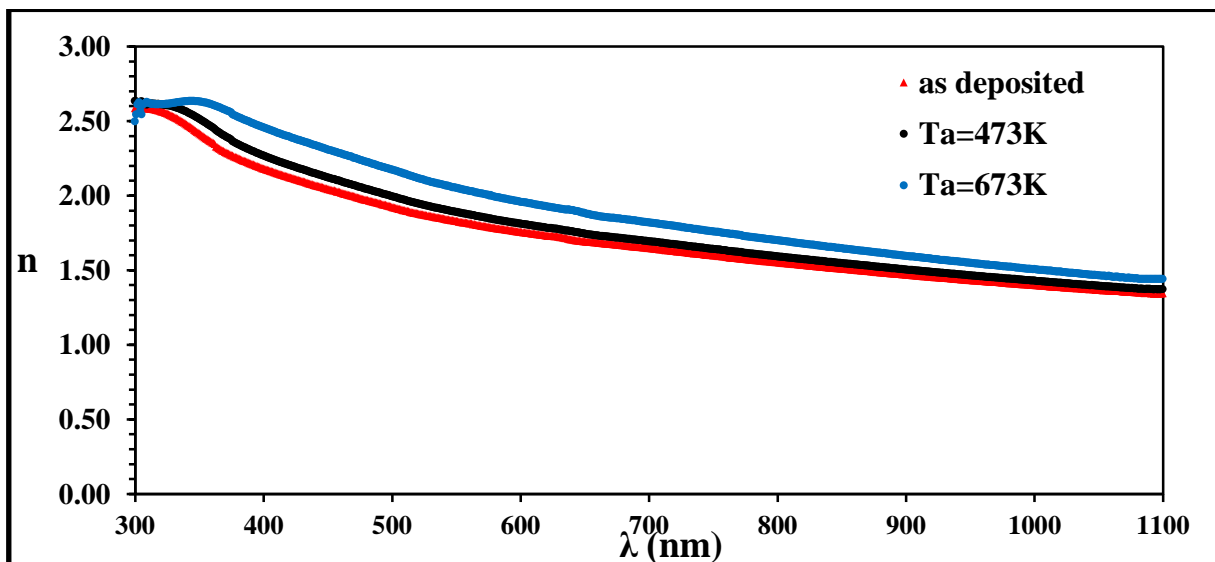


Fig. (6)The variation of refractive index with the wavelength for as deposited and annealed ZnO films.

The real and imaginary parts of dielectric constant were evaluated using the formulas <sup>[17]</sup>:

$$\epsilon_r = n^2 - k^2 \dots\dots\dots 8$$

$$\epsilon_i = 2nk \dots\dots\dots 9$$

The variation of the real and imaginary parts of the dielectric constants values versus wavelength have been shown in figures (7 and 8) for as deposited and annealed ZnO films on glass. Their value are decreased with wavelength more than 500nm. The variation of the dielectric constant depends on the value of the refractive index. By contrast, the dielectric loss depends mainly on the extinction coefficient values which are related to the variation of absorption.

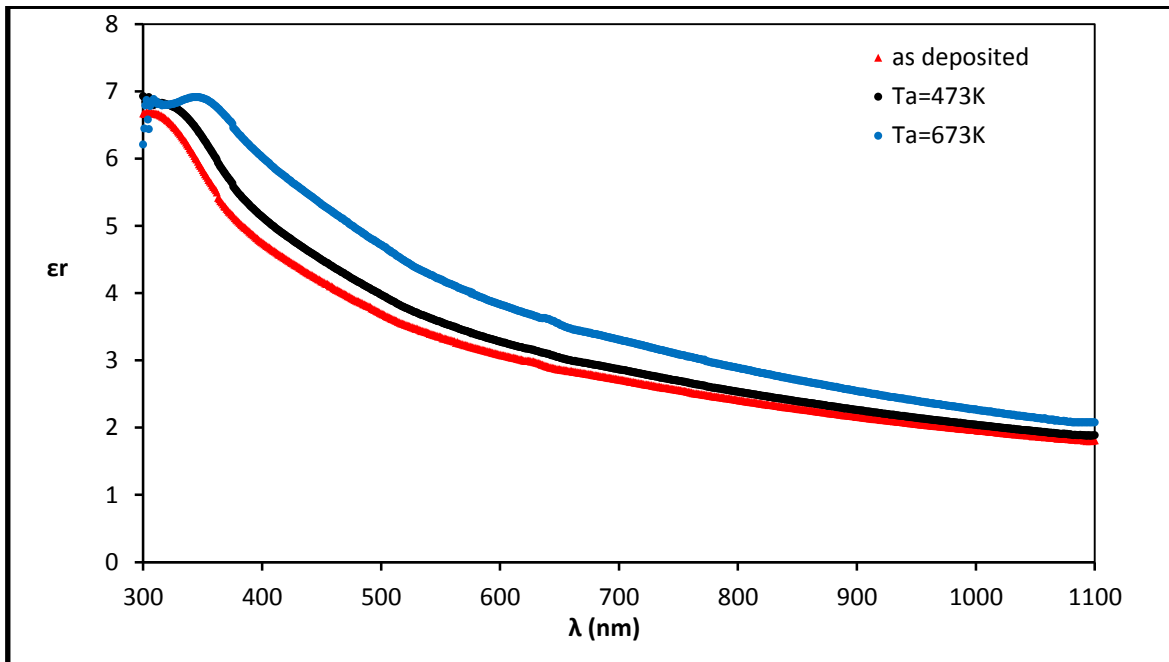


Fig.(7) The variation of  $\epsilon_r$  with the wave length for as deposited and annealed ZnO films.

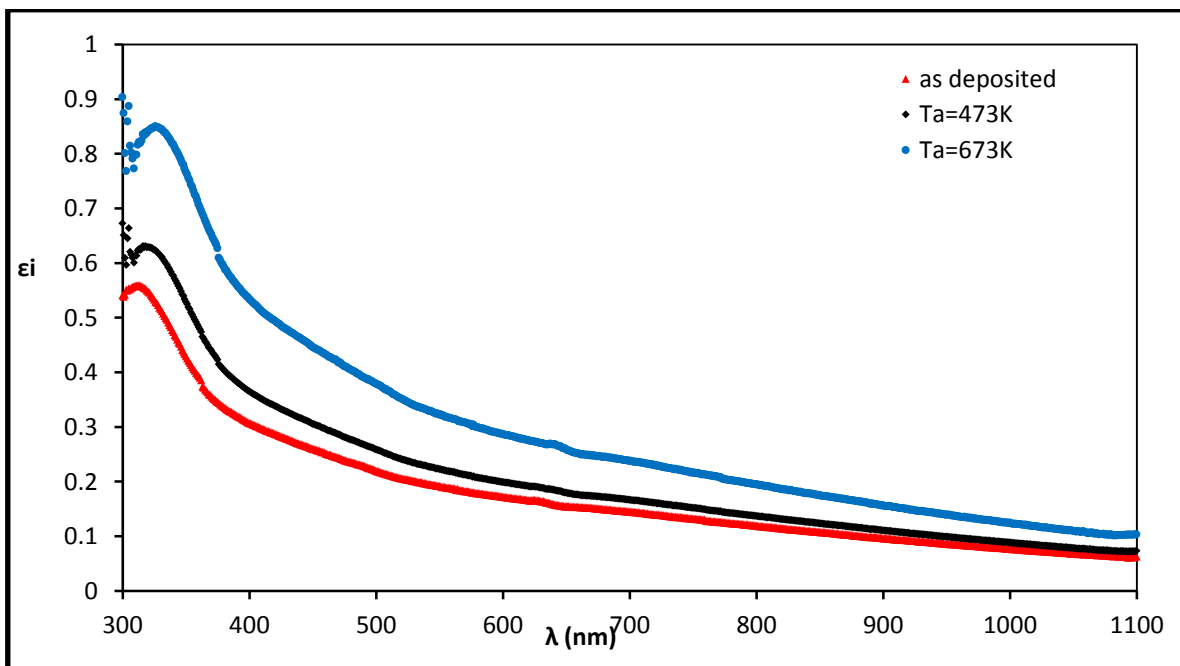


Fig. (8) The variation of  $\epsilon_i$  with the wave length for as deposited and annealed ZnO films.



Table (1) shows the optical constants for as deposited and annealed ZnO films on glass at  $\lambda = 500$  nm and the optical parameters values for these prepared samples. This Table illustrates that the values of  $\alpha$ ,  $k$ ,  $n$ ,  $\epsilon_r$  and  $\epsilon_i$  increase with annealing, whereas  $T$  and  $E_g$  are opposite i.e., they decrease with annealing.

Table (4) The optical parameters at  $\lambda = 500$  nm and  $E_g$  for as deposited and annealed ZnO films.

| $T_a$ (K)    | T%    | $\alpha$ ( $\text{cm}^{-1}$ ) | K     | n     | $\epsilon_r$ | $\epsilon_i$ | $E_g$ (eV) |
|--------------|-------|-------------------------------|-------|-------|--------------|--------------|------------|
| as deposited | 80.63 | 14355                         | 0.057 | 1.924 | 3.698        | 0.220        | 3.26       |
| 473          | 78.30 | 16314                         | 0.065 | 1.995 | 3.976        | 0.259        | 3.20       |
| 673          | 72.07 | 21839                         | 0.087 | 2.171 | 4.707        | 0.378        | 3.14       |

## Conclusions

Optical properties for as deposited and annealed ZnO films, prepared by pulse laser deposition technique have been studied. The outcome of this investigation can be summarized as follows:

- ZnO films were convert from amorphous to hexagonal polycrystalline structure when annealed at 473 K under  $10^{-3}$  mbar vacuum for one hour and with increasing annealing temperature to 673 K leads to increase the crystallinity
- It is shown that the grain size increases as the annealing temperature increases, which lead to decrease the non-uniform strain.
- It can also see from table (1) an increasing in  $d_{hkl}$  with increasing  $T_a$  i.e., slightly shift in  $2\theta$  to lower values, i.e increase in lattice constant which effect on the energy gap.
- The transmittance increases with increasing wavelength while it decreases with annealing.
- The energy gap decreases from 3.26 eV to 3.14 eV with annealing.
- The optical constants values(  $\alpha$ ,  $k$ ,  $n$ ,  $\epsilon_r$  and  $\epsilon_i$  ) increase with annealing.

## References

- [1] A.D.A. Buba and J.S.A. Adelabu, Optical and Electrical Properties of Deposited ZnO Thin Films, The pacific Journal of Science and Technology.11 (2010) 429-434.
- [2] D. Cornejo Monroy, J.F. Sanchez-Ramirez, M.Herrera-Zaldivar and u. Pal,Effect of Deposition parameters on the Optical and Microstructura Characteristics of Sputtered deposited nanocrystalline ZnO Thin Films, Revista Mexicana De Fisica. 53(2007),23-28.
- [3] R.Sharma, P.K. Shishodia, A. Wakahara and R.M. Mehra,Investigations of Highly Conducting and Transparent Sc Doped ZnO Films Grown by the Sol-gel process, Materials ciencia- Poland. 27(2009),225-237.
- [4] Xu Y. N., Ching W. Y., "Electronic, optical, and structural properties of some wurtzite crystals", Physical Review B 48, 4335-4351 (1993)
- [5] J. Dean "Lange`s Handbook of chemistry" Hill Book Company,(1980).
- [6] Y.F.Mei, G.G.Siu, Ricky K.Y.Fu, Paul K.Chu,Z.M. Li, Z.K. Tang, Room-temperature electrosynthesized ZnO thin film with strong (002) orientation and its optical properties, Applied Surface Science. 252 (2006) 2973-2977.
- [7] B. J. Lokhande, M.D.Uplane, Structural, Optical and Electrical Studies on Spray Deposited Highly Oriented ZnO Films, Applied Surface Sciences.167.(2000) 243-246.
- [8] T.C.Zhang, Y.Guo, Z.X.Mei, C.Z.Gu, and X.L.Du,Visible-blind Ultraviolet Ohotodetector Based on Double Heterojunction of n-ZnO / Insulator -Mg/p-Si, Applied Physics
- [9] L. Kukreja, B. Singh and P. Misra, "Pulsed Laser Deposition of Nanostructured Semiconductors", Centre for Advanced Technology, India, (2006).

- [10] B. Warren, X-ray Diffraction, Addison-Wesley Publishing Company, (1969), p. 253.
- [11] V. D. Mote, Y. Purushotham and B.N. Dole "Williamson-Hall analysis in estimation of lattice strain in nanometer-sized ZnO particles" *Journal of Theoretical and Applied Physics* 2012, 6:6.
- [12] JCPDF card No. 96-901-1663
- [13] Cullity B D and Stock S R 2001 *Elements of X-Ray Diffraction*, New Jersey, Prentice Hall
- [14] Z. Rizwan, A. Zakaria, M. Ghazali, A. Jafari, F. Ud Din, and R. Zamiri, *Int. J. Mol. Sci.*, V. 12 ( 2011) P. 1293.
- [15] J. Tauc, "Amorphous and Liquid Semiconductors ", Plenum Press, London and New York (1974).
- [16] S. Aksoy, Y. Caglar, S. Ilican, and M. Caglar, *Optica Applicata*, V. XL, N.1 (2010) P.7
- [17] L. Kazmerski, "Polycrystalline and Amorphous Thin Films and Devices ", Academic Press (1980).